EUROPEAN FUSION DEVELOPMENT AGREEMENT

EFDA–JET–PR(02)25

X. Litaudon, A. Bécoulet, F. Crisanti, R.C. Wolf, Yu. F. Baranov, E. Barbato, M. Bécoulet, R. Budny, C. Castaldo, R. Cesario, C. D. Challis, G. D. Conway, M. R. De Baar, P. De Vries, R. Dux, L.G. Eriksson, B. Esposito, R. Felton, C. Fourment, D. Frigione, X. Garbet, R. Giannella, C. Giroud, G. Gorini, N.C. Hawkes, T. Hellsten, T.C. Hender, P. Hennequin, G.M.D. Hogeweij, G. T. A. Huysmans, F. Imbeaux, E. Joffrin, P.J. Lomas, Ph Lotte, P. Maget, J. Mailloux, P. Mantica, M.J. Mantsinen, D. Mazon, D. Moreau, V. Parail, V. Pericoli, E. Rachlew, M. Riva , F. Rimini, Y. Sarazin, B. C. Stratton, T.J.J. Tala, G. Tresset, O. Tudisco, L. Zabeo and K-D. Zastrow

Progress Towards Steady-State Operation and Real Time Control of Internal Transport Barriers in JET

Progress Towards Steady-State Operation and Real Time Control of Internal Transport Barriers in JET

X. Litaudon[1], A. Bécoulet[1], F. Crisanti[2], R.C. Wolf[3], Y.F. Baranov[4], E. Barbato[2], M. Bécoulet[1], R. Budny[5], C. Castaldo[2], R. Cesario[2], C. D. Challis[4], G. D. Conway[6], M. R. De Baar[7], P. De Vries[7], R. Dux[6], L.G. Eriksson[1], B. Esposito[2], R. Felton[4], C. Fourment[1], D. Frigione[2], X. Garbet[1], R. Giannella[1], C. Giroud[7], G. Gorini[8], N.C. Hawkes[4], T. Hellsten[9], T.C. Hender[4], P. Hennequin[1], G.M.D. Hogeweij[7], G. T. A. Huysmans[1], F. Imbeaux[1], E. Joffrin[1], P.J. Lomas[4], Ph Lotte[1], P. Maget[1], J. Mailloux[4], P. Mantica[8], M.J. Mantsinen[10], D. Mazon[1], D. Moreau[1], V. Parail[4], V. Pericoli[2], E. Rachlew[9], M. Riva[2], F. Rimini[1], Y. Sarazin[1], B. C. Stratton[5], T.J.J. Tala[10], G. Tresset[1], O. Tudisco[2], L. Zabeo[1], K-D. Zastrow[4]
and contributors to the EFDA-JET workprogramme*

[1]*Association EURATOM-CEA, CEA Cadarache, F-13108 St Paul lez Durance, France*
[2]*Associazione EURATOM-ENEA sulla Fusione, Centre Ricerche Frascati, Italy*
[3]*Institut für Plasmaphysik, Association EURATOM-FZJ, D-52425 Jülich, Germany*
[4]*UKAEA-EURATOM Association, Culham Science Centre, Abingdon, OX14 3DB, UK*
[5]*Princeton Plasma Physics Laboratory, P.O. Box 451, Princeton, NJ 08543, USA*
[6]*Max-Planck-Institut für Plasmaphysik, EURATOM-Assoziation, Garching, Germany*
[7]*Associatie EURATOM-FOM, TEC, Cluster, 3430 BE Nieuwegein, The Netherlands*
[8]*Instituto di Fisica del Plasma, EURATOM-ENEA-CNR Association, Milan, Italy*
[9]*Alfven Laboratory, KTH, Association EURATOM/VR, S-10044 Stockholm, Sweden*
[10]*Association EURATOM-TEKES, VTT Chemical Technology, FIN-02044, Finland*
** See annex of J. Pamela et al, "Overview of Recent JET Results and Future Perspectives", Fusion Energy 2000 (Proc. 18th Int. Conf. Sorrento, 2000), IAEA, Vienna (2001).*

Preprint of Paper to be submitted for publication in
Nuclear Fusion

ABSTRACT.

In JET advanced tokamak research mainly focuses on plasmas with internal transport barriers (ITBs), which are strongly influenced by the current density profile. The formerly developed optimised shear regime with low magnetic shear in the plasma center has been extended to deeply negative magnetic shear configurations. High fusion performance with wide ITBs has been obtained transiently with negative central magnetic shear configuration: $H_{IPB98(y,2)}$~1.9, $\beta_N = 2.4$ at $I_p = 2.5$MA. At somewhat reduced performance electron and ion ITBs have been sustained in full current drive operation with 1MA of bootstrap current: $H_{IPB98(y,2)}$~1, $\beta_N = 1.7$ at $I_p = 2.0$MA. The ITBs have been maintained up to 11s for the latter case. This duration, much larger than the energy confinement time (37 times larger), is already approaching a current resistive time. New real-time measurements and feedback control algorithms have been developed and implemented in JET for successfully controlling the ITB dynamics and the current density profile in the highly non-inductive current regime.

INTRODUCTION

Improvement of the tokamak concept in terms of confinement and stability is a crucial challenge that could lead to operating the device in a continuous mode. In a steady-state tokamak reactor the plasma current is entirely sustained by non-inductive current drive means and the self-generated bootstrap current provides a significant fraction of the plasma current. A major challenge remains to extend the high performance regimes obtained in present days tokamaks towards genuine steady-state conditions where the current density profile is non-inductively driven. The development of steady state operational regimes with improved confinement and stability is known as 'advanced tokamak' research (e.g. [1-4]). This paper reports on the recent (2000-2002) progress achieved on JET towards controlled steady-state regime.

In JET, advanced tokamak research mainly focuses on plasmas with Internal Transport Barriers (ITBs), which are strongly influenced by the current density profile [5-6]. ITBs are qualitatively defined as regions in the plasma core where the radial anomalous thermal transport (and/or particle) of the conventional confinement mode (L-mode) is significantly reduced. Moreover, a quantitative ITBs definition has been proposed and successfully applied to characterise the JET ITBs (emergence, strength and space-time evolution) in a wide range of plasma parameters [7]. It was found that the dimensionless local parameter, $\rho_T^* = \rho_s/L_T$ characterises with a low computational cost the ITB features [ρ_s/L_T is the local ion Larmor radius at the sound speed normalised to the (electron or ion) temperature gradient scale length L_T]. An ITB exists when the normalised Larmor radius, ρ_T^*, exceeds some critical value, ρ_{ITB}^*, i.e. $\rho_T^* \geq \rho_{ITB}^*$. A possible interpretation leading to the theoretical relevance of this dimensionless criterion as a local indicator of a bifurcated plasma state is the stabilisation of turbulence by the ExB rotational flow shear. By resorting to a dimensional analysis, it is possible to recast the ExB stabilisation criterion (the E×B shear exceeding a typical linear growth rate) in the form of $\rho_T^* \geq \rho_{ITB}^*$. Dependence of ρ_{ITB}^* on some dimensionless parameters are in principle possible. In practise, a systematic and statistic analysis of 116 JET discharges has shown that the criterion

characterises well the appearance of ITBs with a critical value of $\rho_{ITB}^* = 0.014$ [7]. Once validated, this practical ITB criterion has been used routinely to speed up the identification of the experimental database. In addition, the calculation of this normalised temperature gradient has been implemented in the JET real time system in view of characterising the ITB features and ultimately controlling their dynamics with feedback loops.

The paper is organised as follows. In section 2, the achievement of (transient) high fusion performance with non-monotonic q-profiles (negative central magnetic shear configuration) is reported [8]. The influence of the q-profile in the plasma performance is also stressed. Then in section 3, we will describe the quasi-stationary operation with a high fraction of non-inductive current [9-10]. Finally, the recent and major developments to control in real time with closed feedback loops the local ITB or current profile characteristics are reviewed in section 4 [11].

1. HIGH FUSION PERFORMANCE PLASMAS WITH NEGATIVE CENTRAL MAGNETIC SHEAR

The formerly developed optimised shear regime with low or weakly negative magnetic shear in the plasma center [3, 12-13], has been extended to noticeably negative central magnetic shear configurations [8, 14-17]. The q-profile has been varied using mainly the LHCD during the initial current ramp-up phase of the plasma discharge, prior to the application of the high power heating. Dedicated set of experiments has been performed to reveal the role played by the q-profile in the ITB formation and performance [8]. The magnetic shear in the plasma interior was varied from small and positive in the ohmic preheat case, through weakly to highly negative ('current hole') by increasing the LHCD power and/or optimising the plasma initiation (Fig.1 (left)). In addition, the injected torque in the co-current direction has been systematically varied for each q-profile ($B_o = 2.6$T, I_p~2.2MA). Figure 1 (right) shows the peak value of ρ_{Te}^* applied to the electron temperature profile in the region of 'wide' transport barrier (r/a>0.5), as a function of additional power for the different q-profile and injected torque. The wide ITBs required for high fusion performance are formed close to the low order rational q = 2 surface for both monotonic [18] and non-monotonic q-profiles [19]. The plasmas with an LHCD prelude tend to provide a 'stronger' electron ITB (e.g. larger value ρ_{Te}^*) than the ohmic preheat cases. This observation is attributed to the reduction of the magnetic shear at the location of the low order rational safety factor surface (e.g. q = 2) which is expected to be favourable for the ITB formation and performances [20-21]. Firstly, the high wavenumber ITG/TEM growth rates are decreased when lowering the magnetic shear, as recently discussed for the JET discharges by Garbet et al [21]. Secondly, turbulence simulations also indicate that a low magnetic shear close to low order rational q-surfaces favours the development of a region without any low wave number resonant surface [21].

Following this approach but at higher toroidal field ($B_o = 3.45$T), high fusion performance has been achieved with negative central magnetic shear with a minimum q value, q_{min}, approaching two (Fig. 2 (left)) [8]. The LH power (2-3MW) was applied soon after the plasma initiation until

the main heating phase. A narrow ITB is first visible on the electron temperature profile during the LHCD prelude phase, which persists during the early part of the main heating phase. Then, a wide ITB with very steep gradient develop on the thermal pressure profiles, and is thought to be triggered when q_{min} reaches two. ITBs at large plasma radius contribute significantly to the enhancement of fusion performance: total neutron yield, $R_{NT} = 4.1 \times 10^{16}$ neutrons/s, $H_{ITER\text{-}89P} \sim 3.3$, $H_{IPB98(y,2)} \sim 1.9$, $\beta_N = 2.4$ at $I_p = 2.5$MA ($q_{95} = 4.5$). The transient high performance phase is ended with a large ELM followed by a disruption (global pressure n = 1 kink mode instability). A further increase in performance will require the pressure profile to be further broadened by extending the radius of ITB. More recent experiments were carried out in 2002 (campaign C5) to move outwards the q = 2 low shear magnetic shear region by ramping-up the plasmas current up to 3.8MA ($q_{95} = 2.9$).

Finally, the performance of the two types of JET ITB regimes are compared on Figure 2 (right) where the peak neutron rate is plotted versus the additional power for weak and negative central magnetic shear configuration. Heating power in the range of 16MW is required to generate wide transport barrier and high fusion yield in the negative central magnetic shear configuration, instead of 20MW in the weak magnetic shear cases [8].

3. DEVELOPMENT OF ITB PLASMAS WITH STEADY-STATE POTENTIAL

An approach towards stationary operation has been investigated by maintaining the LH power during the high power ELMy H-mode phase in order to slow down the current profile evolution [9-11, 22-24]. Figure 3 shows one of the longest pulse with LH power combining an ELMy H-mode edge (high frequency type III ELMs) and core transport barrier sustained with a loop voltage, V_s, approaching zero (Ip = 2MA, $q_{95} = 5.5$, $H_{ITER\text{-}89P} \sim 2$, $H_{IPB98(y,2)} \sim 1$, Ip = 1.1, $\beta_N = 1.7$ at B_o = 3.45T). Successful coupling of the LH waves during the H-mode phase has been obtained by increasing the density at the antenna mouth by locally injecting CD_4 gas [24-25]. The line-averaged electron density measured close to the edge transport barrier with the type III ELM activity keeps a constant value during the high power phase at typically $1.5 \times 10^{19} m^{-3}$. The particle sources at the edge are determined by the plasma recycling at the wall and the injection of CD4 gas. In this discharge, the electron ITB is maintained during 11s from the LH preheat phase up to the pre-programmed end of the power waveforms. This is the longest discharge during which an ITB has been sustained on JET and this duration corresponds approximately to 37 energy confinement times, τ_E. Those ITB durations become comparable to the volume averaged resistive current diffusion time evaluated with the local neo-classical conductivity profile. The ITB also observed on the ion temperature, electron density and toroidal rotation profiles is sustained during the high power phase (~8s, ~27 τ_E) starting at t = 4.2s. The core electron density is rising up to $n_{eo} = 6.0 \times 10^{19} m^{-3}$ **mainly due to the core NBI fuelling** and the line-averaged density normalised to the Greenwald density is 0.55. The duration of this type of discharge is close to the JET technical operational limits fixed by the maximum duration of application of the full NBI power and the high toroidal field operation.

The target q-profile is non-monotonic with $q_{min} \sim 3$ at r/a~0.5 as inferred from the EFIT code

constrained by MSE measurements or FIR polarimetry data. In the high power phase, the q-profiles keep a non-monotonic shape with q_{min} maintained above 2 at mid-radius. The FIR polarimetry data indicates that q_{min} is at mid-radius and slowly decreases from 3 down to approximately 2.5 just at the end of the high power phase. The internal inductance, l_i, keeps a low value (~0.8) up to the end of the high power phase and weakly evolves by less than 10%. The slow evolution of the q-profile, in particular the location and value of q_{min}, allows to maintain the ITBs inside mid-plasma radius, i.e. in the weak or negative magnetic shear region, without reaching the disruptive ideal n=1 kink limit. The q-profile evolution is slowed down thanks to the high fraction of non-inductive current reaching up to 90% of the total current as calculated by TRANSP or CRONOS [26-27]. The non-inductive current fraction is fairly constant with time: when the electron density is increased the LH and NB non-inductive currents are both reduced but this effect is partly compensated by the rise of the bootstrap current. The self-consistent CRONOS simulations of the various non-inductive currents with the 2-D equilibria indicate that the off-axis bootstrap current rises up to 1.0MA, the NBCD varies between 0.2-0.6MA, while the LHCD deduced from ray-tracing coupled to 2-D Fokker-Planck modelling is in the range of 0.4-0.8MA (Fig. 3 (right)) [10]. The LH ray-tracing simulations during the high power phase show that the LH power is absorbed in a broad off-axis region thanks to the strong electron Landau damping with high electron temperature.

The possibility to sustain the ITB characteristics offers the opportunity of quantitatively studying the particle and impurity transport. Such studies require that the regime is maintained on time duration at least of the order of the particle confinement time (several τ_E). These studies have shown that the core impurity transport follows the trends predicted by the neo-classical theory : high Z-impurity accumulation with strong peaking of the density profile competing with the screening effect expected from high ion temperature gradient [28-29]. In the experiment shown on Fig. 3, the screening effect is either too localised and/or not strong enough to prevent the central accumulation of the metallic impurity. The high-Z impurity accumulation (central Nickel density rising up to $4 \bullet 10^{17} m^{-3}$) leads to a core radiative collapse (t=11.1s) in which energy and density are expelled. The radiative power density in the plasma core (r/a<0.3) increases up to $140 kW/m^3$ (at t=11.1s) which is indeed approaching the conducted electron power density. Control of the impurity content will be investigated either by triggering core MHD activity or by controlling the density and temperature profiles (c.f. section 4).

One of the surprising results of this experiment is that the ITB is reformed immediately after the core MHD (t≈6.7s) or radiative (t≈11.1s) collapses. These collapses affect on a fast time scale the pressure, toroidal rotation and radial electric field profiles but the q-profile, evolving on a longer time scale, keeps a non-monotonic shape. Simulations shown on Fig.4 performed with the electrostatic linear gyrokinetic code, KINEZERO [30], indicate that the ion instabilities driven by the ITG and the trapped electron modes are suppressed in the region of negative magnetic shear [10, 31-33]. Therefore, the direct reduction or stabilisation of the turbulence through the q-profile is invoked to explain the rapid recovery of the ITB to various collapses as long as these perturbations affect only weakly the low or negative magnetic shear region.

One of the challenges for the viability of steady-state plasmas consists in successfully combining the H-mode confinement with the ITB characteristics. High performance ITB discharges occur typically at power levels well above the L to H mode transition and even above the type-III to type-I ELM transition. When a transition to large amplitude ELMs occurs, the ITB is either lost with a back transition to a lower confinement state or the whole plasma becomes unstable leading to a major disruption. Although the total applied power is at least a factor two above the power threshold to trigger large amplitudes ELMs, the ELM's activity keeps a mild type-III behaviour in these highly non-inductive current discharges even without injecting radiative gases for edge cooling. The mitigation of the ELM's activity has been interpreted by analysing the role played by the broad q-profile with low l_i values (l_i~0.7-0.8) on the threshold conditions from type III to type I ELM [34-35]. A larger current fraction at the plasma 'edge' in the ITB discharges compared to the similar standard H-mode ones could prevent a transition to type-I ELM by changing the edge MHD stability conditions. To characterise the edge current fraction, the internal inductance (l_i), the edge magnetic shear (sh_{95}) and the polarimetry measurements (in particular the line of sight close the edge, R~3.75m) have been simultaneously used. It was indeed checked that the ITB discharges with a high fraction of non-inductive current have larger edge current compared to the standard H-mode regime in agreement with the polarimetry measurements together with the lower values of l_i and sh_{95} [34-35]. The broad current profile with a larger edge current fraction (compared to the H-mode regime) is sustained throughout the high power phase since a large fraction of off-axis non-inductive current is continuously driven in these long duration ITB discharges.

This edge issue has been further investigated in the 2002 experimental campaign in similar operating conditions but at high triangularity, δ~0.45, where the ELM activity is expected to be even stronger. So far JET ITB experiments were mainly performed at reduced values of triangularity (δ~0.2). The recent modification of the divertor geometry (the septum part of the MKII Gas Box has been removed) has allowed ITB operation with plasma equilibria at triangularity closer to the values envisaged for ITER advanced mode of operation. The ELM behaviour has been changed (at fixed deuterium gas injection rate) by varying the plasma current once the negative central magnetic shear configuration was established. In the experiment shown on Figure 5, the full power is applied on a 2MA current plateau where type I ELM activity is triggered. Then, the current is raised by 0.3MA, inducing an increase of the edge current ('skin effect') that destabilises the n=1 peeling modes. As a consequence, the type I ELM activity is suppressed: confirming the role played by the edge current density on the ELM behaviour.

4. REAL-TIME FEEDBACK CONTROL OF THE ITB PLASMAS FOR STEADY-STATE OPERATION

New real-time measurements and control algorithms have been developed and implemented for controlling the ITB dynamics and the current density profile: confinement parameters, temperatures, particle and q-profiles are now available in real-time.

A double-loop feedback control with combined ICRH and NBI has been first applied in the non-inductive current drive operational regime described in section 3 [11]. The NBI power controls the total neutron yield, R_{NT}, at a given reference and consequently the total bootstrap current fraction through the control of the core plasma pressure. In addition, the ICRH is simultaneously used as an actuator to control the normalised electron temperature gradient in the barrier region, i.e. the maximum value of $\rho_{Te}^* = \rho_s/L_{Te}$ (Fig.6 (left)). For this purpose, the local ITB criterion [7] characterising the space-time evolution of the ITBs has been calculated in the real time system from the ECE radiometer data. The LHCD power is maintained in a pre-programmed way to provide the correct q-profile ensuring the core confinement and MHD stability. In the example shown on Figure 6 (left), the values of the maximum ρ_{Te}^*, and of the neutron rate are maintained constant respectively at 0.025 and 0.9×10^{16} neutrons/s. The active control of the temperature gradient provides an indirect way of acting on the current density profile through the bootstrap current (I_{Boot}~0.9MA, I_p = 1.8MA). The control of the ITB is applied during 7.5s until the end of the pre-programmed power waveform envelope within which the NBI and ICRH powers are allowed to vary. During the control phase, the plasma parameters of the discharge are fairly stationary with mild and continuous ELM activity. Thanks to the real time control of the ITB characteristics, the improved confinement state is maintained in a more reproducible and stationary manner, e.g. avoiding the occurrence of the core collapses.

Recent efforts have been made in order to develop an algorithm which provides a measurement of the q-profile in real-time and allows feedback control [36-37]. The algorithm uses as inputs the signals of the magnetic and interfero-polarimeter diagnostics. The approach described in the previous paragraph is based on decoupled loops controlling the core pressure and temperature gradient at two radii with devoted actuators. A 'model-based' profile control scheme is now followed, in which more information on the spatial structure of the system is taken into account by retaining its distributed nature, and considering the non-local interaction between various quantities through a diffusion-like operator [38]. To validate this 'model based' technique a direct control of the safety factor profile has been tried using LHCD as the only actuator. The experiment was performed during an extended LHCD prelude phase at low density and beta. The plasma current was fixed at 1.5MA, in order to be close to a purely non-inductive current drive regime with the available LH power and thus have a larger flexibility for obtaining weak shear q-profiles. The feedback control was performed on five points of the q-profile located at fixed normalised radii (r/a=0.2, 0.4, 0.5, 0.6, 0.8) and the reference q-profile is reached within 4s (Fig.6 (right)). To reach the pre-set reference q-profile the controller minimises in the least square sense the difference between the five target q-values and the real-time measurements. Modelling of the current diffusion evolution using the CRONOS code [26-27] confirms that a stationary state with a flat toroidal electric field profile was reached (the resistive time is around 4s in these experiments). The simulations also indicate that 0.9MA of non-inductive current is driven by the LH waves absorbed at mid-radius**.**

The successful experiment reported here should be considered as a 'proof of principle'. In the

near future, this general 'model-based' approach will be implemented in view of controlling high-β, high-bootstrap fraction, ITB discharges where pressure and current density profiles are strongly non-linearly coupled.

CONCLUSION AND PROSPECTS

Using off-axis LH current drive, the formerly developed Optimised Shear regime [3] with low or weakly negative magnetic shear in the plasma centre has been extended up to noticeably negative central magnetic shear configurations [8]. To conclude, the performances of these ITB plasmas quantified by the product of the $H_{ITER89P} \times \beta_N$ have been plotted on figure 7 versus the total injected energy, i.e. applied power times the discharge duration. This graph summarises the results achieved with ITB plasmas and negative central magnetic shear configuration over the JET experimental period extending from June 2000 up to June 2002 (experimental campaigns C1 to C5):

- High performances with wide ITB (r/a ~0.6) triggered when q_{min} reaches a low order rational surface (two) have been achieved transiently (during ~2 τ_E) at $H_{ITER-89P}$~3.3, $H_{IPB98(y,2)}$~1.9, $\beta_N = 2.4$ ($I_p = 2.5$MA, $B_o = 3.45$T, $q_{95} = 4.5$) with 40% of bootstrap current and 55% of non-inductive current [8].
- Quasi-stationary regimes with narrower ITB (r/a ~0.4) and mild type III-ELM activity have been sustained on a resistive time scale (~37 τ_E) at $H_{ITER-89P}$~2, $H_{IPB98(y,2)}$~1, $\beta_N = 1.7$, ($I_p = 2$MA, $B_o = 3.45$T, $q_{95} = 5.5$) with 50% of bootstrap (1MA) and up to 100% of non-inductive current [9-10].

In addition, the feasibility to control in real time the ITB characteristics (e.g. the electron temperature gradient at the ITB location) with feedback loops has been demonstrated in the highly non-inductive current regime. The sustainement and the real time control of the ITBs in full current drive operation with a significant fraction of bootstrap current represent a major milestone towards the definition and viability of the steady-state tokamak operation.

Nevertheless, despite these favourable results for the advanced mode of operation, plasma performances quantified for instance in terms of the normalised pressure (e.g. β_N) of the JET non-inductive quasi steady-state regime should be further increased. Figure 8 summarises the results obtained so far in the JET ITB regime where β_N is plotted versus the total applied power at various toroidal field. Thanks to the enhanced capabilities of the improved heating systems (NBI and ICRH) for the future experimental campaigns, we are aiming at β_N ~3 for steady-state ITB plasmas [39]. One obvious route to pursue to reach this goal in quasi-steady state consists in extending the radius of the ITB for embracing a larger plasma volume with reduced transport. We have shown that wide ITB with steep gradient, could be formed when the low magnetic shear region is moved outwards close to low order rational q-surface (e.g. $q = 2$). A major challenge remains to sustain and control towards stable steady-state conditions the characteristics of the wide ITBs together with the required q-profile for confinement and stability. The real time measurements of the kinetics and magnetics profiles together with the 'model-based' feedback control algorithms will be extensively used in future experimental campaigns in view of further increasing the plasmas fusion performance in a quasi-steady state manner. In addition,

effort will be pursued to develop a non-inductive mode of operation in highly shape plasmas at high triangularity (δ~0.5) as requested in the present ITER design.

ACKNOWLEDGEMENTS:

This work has been performed under the European Fusion Development Agreement (EFDA). It is a pleasure to acknowledge the contributors to the EFDA-JET work programme, in particular those involved in the Task Force S2 and in the Task Force H, as well as the UKAEA, operator of the EFDA-JET facility, and the EFDA Close Support Unit in Culham.

REFERENCES

[1]. Taylor T.S. 1997 Plasma Phys. Control. Fusion **39** B47
[2]. Litaudon X. 1998 Plasma Phys. Control. Fusion **40** A251
[3]. Gormezano C. 1999 Plasma Phys. Control. Fusion **41** B367
[4]. Wolf R.C. 2003 Plasma Phys. Control. Fusion **45** R1
[5]. Special issue on *"Advanced tokamak research in EFDA-JET during the 2000-2001 experimental campaigns"* 2002 Plasma Phys. Control. Fusion 44 1031
[6]. Bécoulet A. et al 2001 Plasma Phys. Control. Fusion **43** A395
[7]. Tresset G., Litaudon X., Moreau D. and Garbet X. 2002 Nucl. Fusion **42** 520
[8]. Challis C.D. et al 2002 Plasma Phys. Control. Fusion **44** 1031
[9]. Crisanti F. et al 2002 Phys. Rev. Letters **88** 145004-1
[10]. Litaudon X. et al 2002 Plasma Phys. Control. Fusion **44** 1057
[11]. Mazon D. et al 2002 Plasma Phys. Control. Fusion **44** 1087
[12]. JET Team (prepared by Gormezano) 1999 Nucl. Fusion **39** 1875
[13]. Söldner F.X. et al 1999 Nucl. Fusion **39** 407
[14]. Challis C.D. et al 2001 Plasma Phys. Control. Fusion **43** 861
[15]. Hawkes N. et al 2001 Phys. Rev. Lett.**87** 115001
[16]. Huysmans G.T.A. et al 2001 Phys. Rev. Lett. **87** 245002
[17]. Tala T.J.J. et al 2002 Plasma Phys. Control. Fusion **44** 1181
[18]. Joffrin E. et al 2002 Nucl. Fusion **42** 235
[19]. Joffrin E. et al 2002 Plasma Phys. Control. Fusion **44** 1739
[20]. Garbet X., Bourdelle C., Hoang G.T. et al 2001 Phys. Plasmas **8** 2793
[21]. Garbet X. et al *2002* 'Micro-stability and Transport Modelling of Internal Transport Barrier on JET' proc 19th Int Conf. (Lyon 2002) (Vienna : IAEA)
[22]. Mailloux J. et al 2002 Phys. Plasmas **9** 2156
[23]. Castaldo C. et al 2002 Phys. of Plasmas **9** 3205
[24]. Tuccillo A. et al 2001 RadioFrequency Power in Plasmas (proc. 14th Top. Conf. Oxnard, CA, 2001) vol. **595** (New York : American Institute of Physics ed T.K. Mau and J. de Grassie) 209

[25]. Pericoli V. et al 2002 'Progress towards internal Transport Barriers at high plasma density sustained by pure electron heating and current drive in the FTU tokamak' submitted to Nucl. Fusion

[26]. Basiuk V. et al 2002 'Simulations of steady-state scenarios for Tore Supra using the CRONOS code' submitted to Nucl. Fusion

[27]. Hoang G.T. et al 2002 'Confrontation of Heat Transport Models Against Tore Supra and JET High Performance Discharges' proc 19th Int Conf. (Lyon 2002) (Vienna : IAEA)

[28]. Dux R. et al 2001 Proc. 28th Eur. Conf. Madeira, vol 25A (EPS) 505

[29]. Dux R. et al 'Accumulation of impurities in advanced scenarios' J. of Nucl Mat. (in press)

[30]. Bourdelle C., Garbet X., Hoang G.T., Ongena J., Budny R.V. 2002 Nuc. Fus. **42** 892

[31]. Eriksson L.-G. et al 2002 Phys. Rev. Lett. **88** 145001-1

[32]. Fourment C., Hoang G.T., Eriksson L.-G, Garbet X., Litaudon X. and Tresset G, 2003 Plasma Phys. Control. Fusion **45** 233

[33]. Esposito B. et al 'Correlation between magnetic shear and ExB shear flow on JET ITBs' in Proc. 29th Eur. Conf. on Plasma Physics and Controlled Fusion, 17-21 June 2002, Montreux (EPS) Vol. 26B (http://crppwww.epfl.ch/eps2002/)

[34]. BÈcoulet M. et al 2002 Plasma Phys. Control. Fusion **44** A103

[35]. Sarazin Y. et al 2002 Plasma Phys. Control. Fusion **44** 2445

[36]. Mazon D. et al 'Real-time control of pressure and current profile in JET' in Proc. 29th Eur. Conf. on Plasma Physics and Controlled Fusion, 17-21 June 2002, Montreux (EPS) Vol. 26B (http://crppwww.epfl.ch/eps2002/)

[37]. Zabeo L. et al 2002 Plasma Phys. Control. Fusion **44** 2483

[38]. Moreau D. et al 'Real Time control of Internal Transport Barriers in JET' Proc. of the 3nd IAEA TCM on Steady State Operation of Magnetic Fusion Devices, May 2002 submitted to Nucl. Fusion.

[39]. Pamela J., Stork D., Solano E. et al 2002 Nucl. Fusion **42** 1014

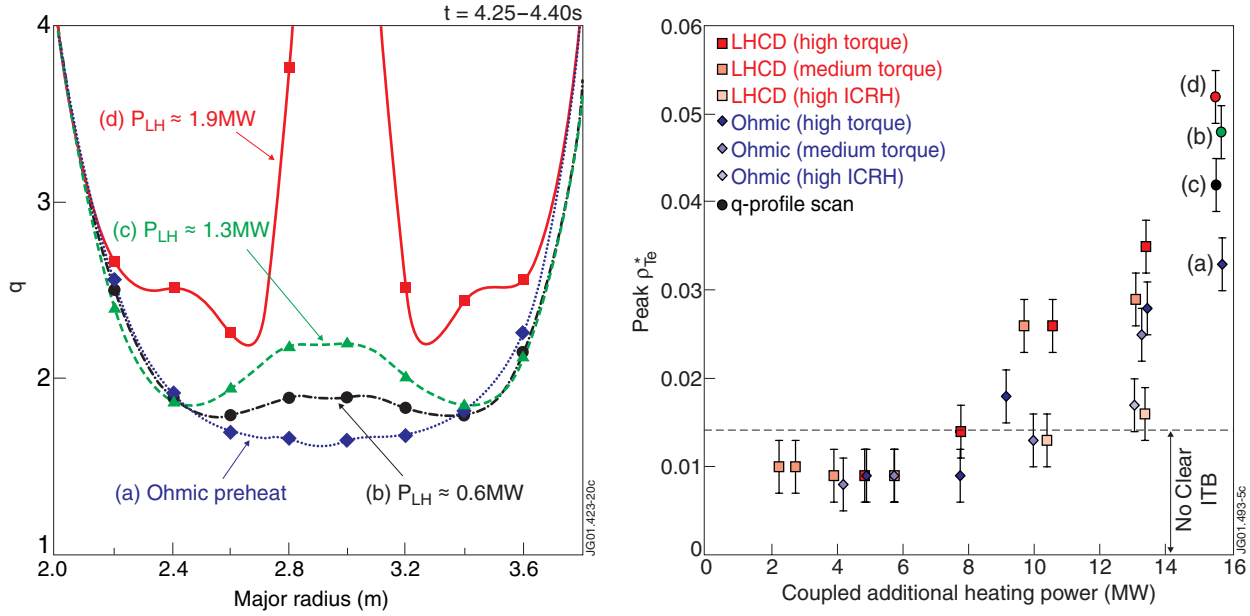

Figure 1: (left) Various target q-profiles prepared with varying LHCD prelude (EFIT equilibrium reconstruction constrained by MSE data). (right) Maximum value of ρ_{Te} versus coupled power for various q-profile and heating scenarios (B = 2.6T); Annotations (a) to (d) refer to the q-profile scan shown on Fig. 1 (left) [8]. In the 'high ICRH' cases the ratio of the ICRH power to the total power is above 50%. This ratio is below 30% in the dominant NBI cases referred as 'high' or 'medium' torque where at a given power level the injected torque has been varied by changing the neutral beam configuration from normal ('medium torque') to tangential ('high torque') beam injection.*

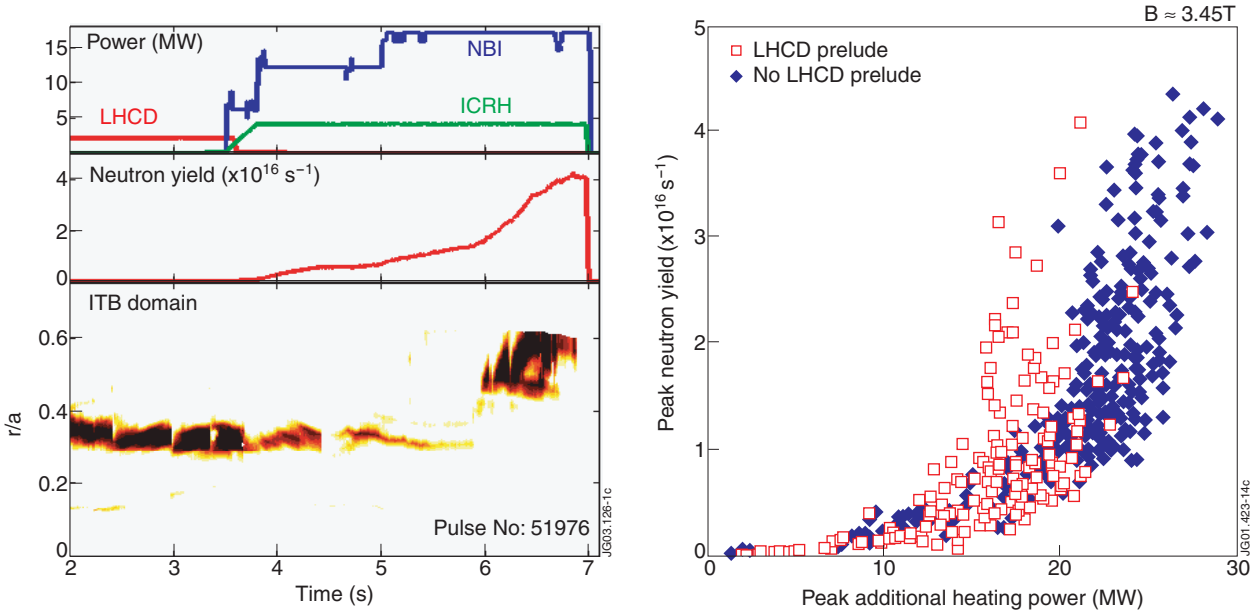

Figure 2: (left) Time evolution of applied powers, neutron yield and ITB radius, as defined in [7], of a high fusion performance negative central magnetic shear discharge (Pulse No: 51976). (right) Peak neutron yield versus additional heating power for the weak and negative magnetic shear magnetic configuration [8] (data from experiments with the JET MKII Gas-Box divertor configuration with the septum part).

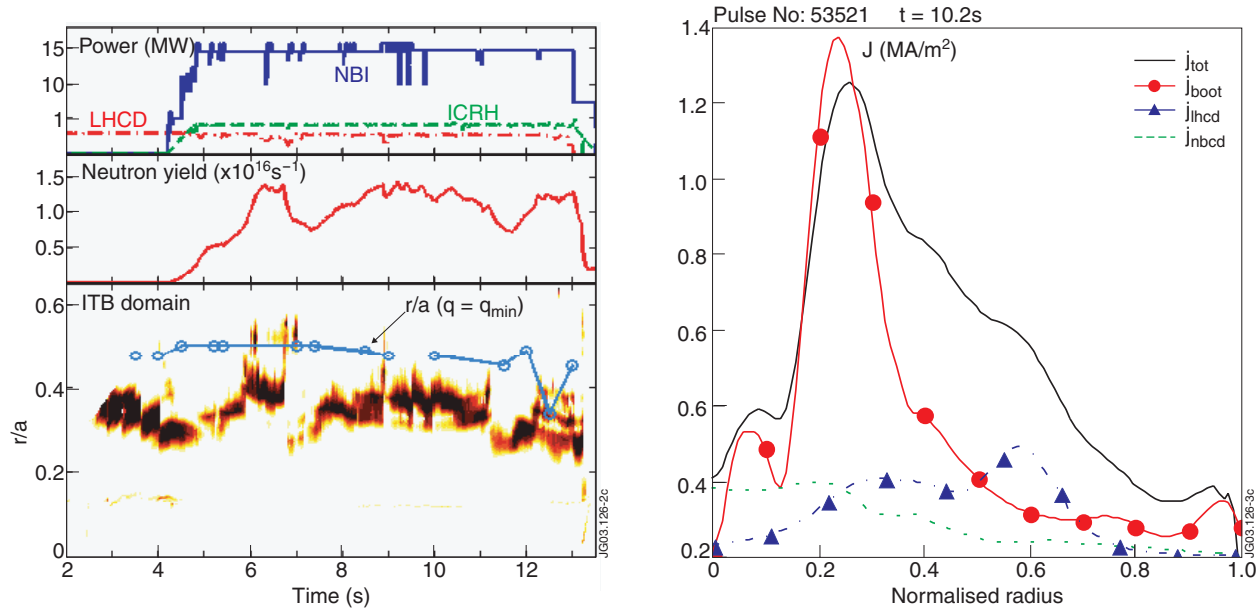

Figure 3: (left) Time evolution of applied powers, neutron yield, ITB radius (as defined in [7]) and q_{min} normalised radius of a highly non-inductive current discharge (Pulse No: 53521). (right) Current density profiles of bootstrap, LH, neutral beam and total deduced from current diffusion simulation performed with the CRONOS code [10].

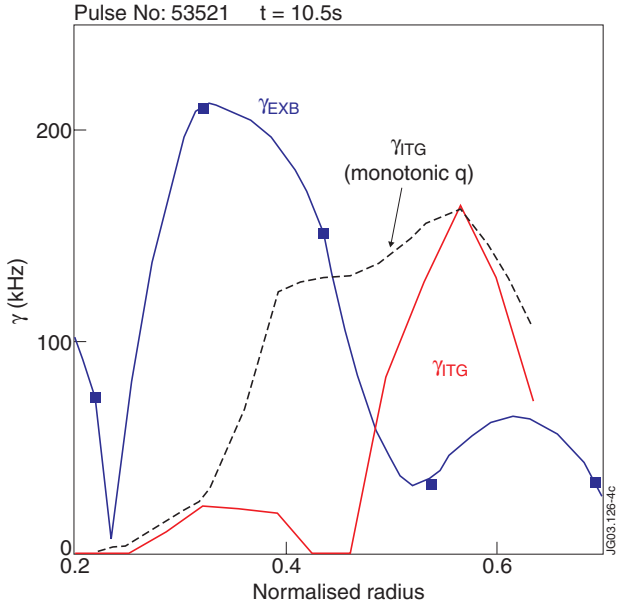

Figure 4 : Linear growth rates, γ, obtained by the gyrokinetic code KINEZERO for the low wavenumbers such as $k_\theta \rho_i$•d 1. The full line corresponds to the simulation performed with the measured non-monotonic q-profile (Pulse No: 53521 at t=10.5s). The dashed line corresponds to a monotonic q-profile case with positive magnetic shear. The radial profile of the ExB shearing rate, γ_{ExB} is shown for comparison.

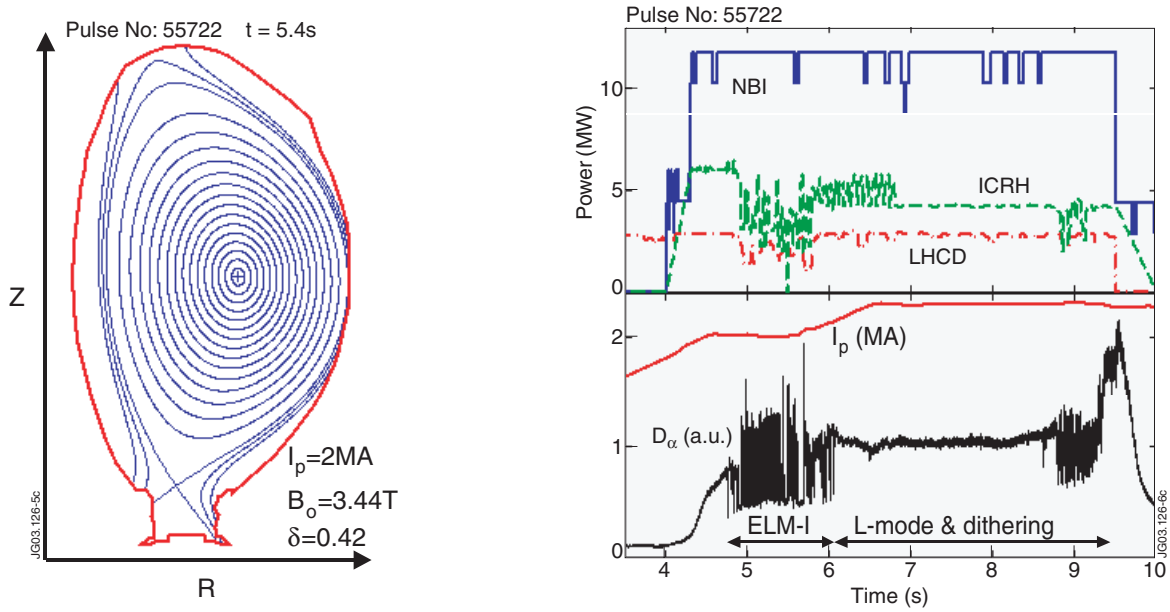

Figure 5: Magnetic equilibria (t=5.4s) and time evolution of coupled powers (NBI, ICRH and LHCD), I_p and D_α-emission in ELM control experiment at high δ (Pulde No: 55722). The ITB is sustained up to t~5s and disappears as a consequence of the Type I ELM activity. Experiment carried out with the MKII Gas Box divertor without the septum part.

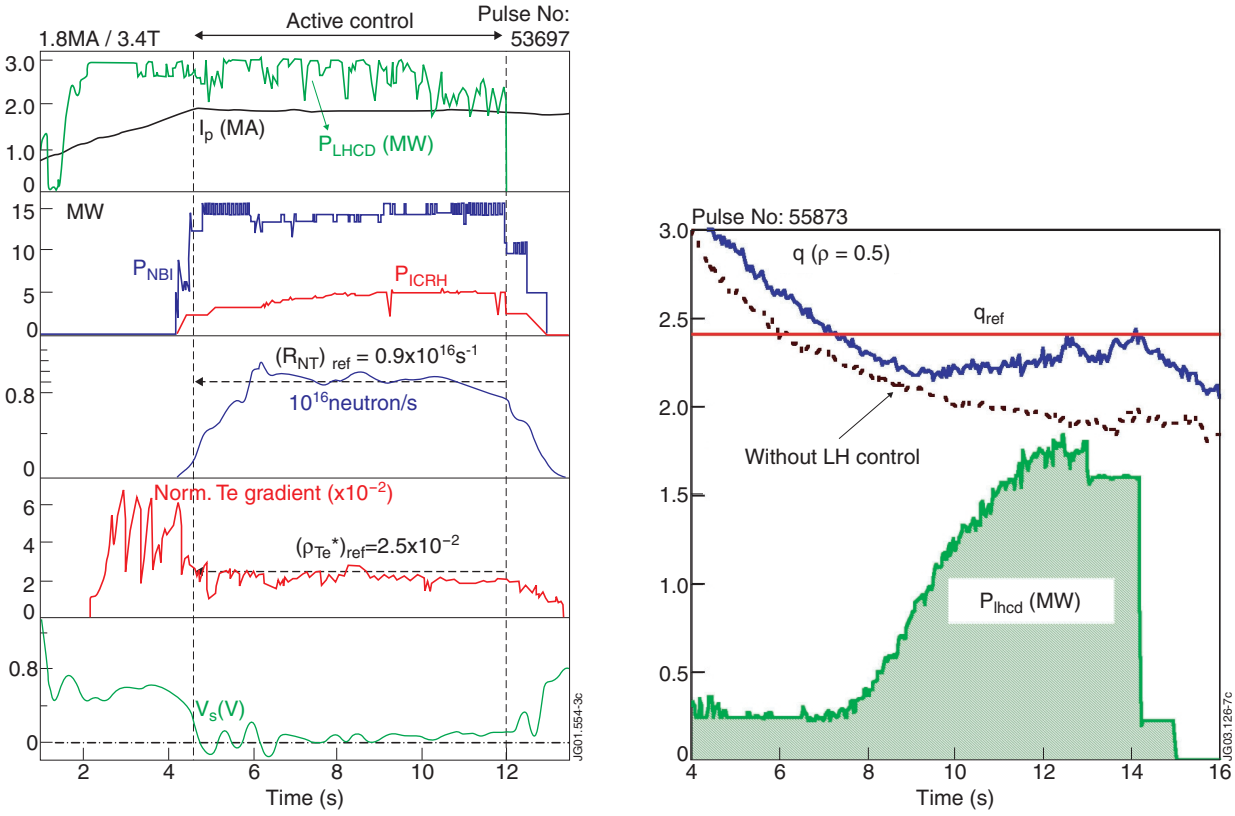

Figure 6: (left) Time evolution of the main parameters of a discharge with combined ρ_{Te} and R_{NT} feedback control using ICRH and NBI powers (Pulse No: 53697) [11]. (right) Real time q-profile control carried out in an extended LHCD prelude phase: time evolution of LHCD power, measured and reference q-values at mid-radius (Pulse No: 55873). A discharge (Pulse No: 55872) without LHCD feedback control is presented for comparison (- - -) [36].*

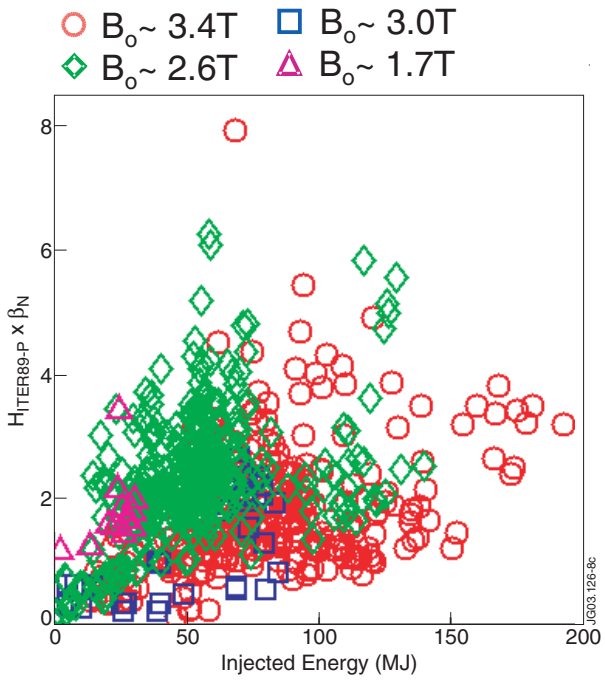

Figure 7 : The maximum value of $H_{ITER89-P} \times \beta_N$ plotted versus the total injected energy at various toroidal fields (B_o~3.4T, B_o~3.0T, B_o~2.6T, B_o~1.7T). The total injected energy is the sum of the injected LHCD, NB and ICRH energy. Each point corresponds to one discharge. The data correspond to ITB experiments carried out during the JET-EFDA experimental campaigns (C1 to C5) from June 2000 up to June 2002.

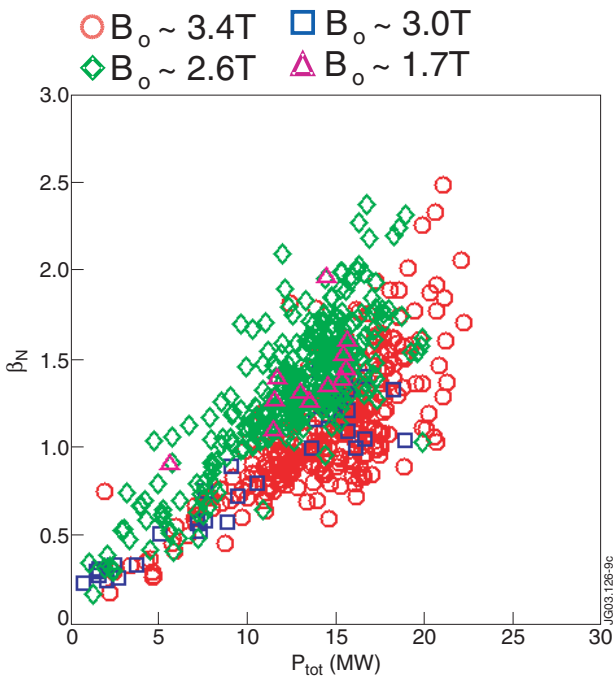

Figure 8 : Normalised (thermal and non-thermal) pressure, β_N, versus the total injected power, P_{tot} at various toroidal fields (B_o~3.4T, B_o~3.0T, B_o~2.6T, B_o~1.7T). The total injected power is the sum of the LHCD, NBI and ICRH powers. Each point corresponds to one discharge. The β_N and P_{tot} values have been obtained at the time of the maximum value of the neutron yield. The data correspond to ITB experiments carried out during the JET-EFDA experimental campaigns (C1 to C5) from June 2000 up to June 2002.